



Effect of Copolymer Composition on the Oxygen Transport Properties of Sulfonated Poly(arylene ether sulfone) and Sulfonated Poly(sulfide sulfone) PEMs

Lei Zhang, Christina Hampel,^a and Sanjeev Mukerjee^z

Department of Chemistry and Chemical Biology, Northeastern University,
Boston, Massachusetts 02115, USA

Mass transport properties were investigated by means of the chronoamperometry method for a series of sulfonated poly(arylene ether sulfone) (SPES) membranes and sulfonated polysulfide sulfone (SPSS) polymers of various ion exchange capacities (IEC) at a Pt (microelectrode)/proton exchange membrane (PEM) interface. The temperature and pressure dependence of oxygen transport parameters show similar trends for the SPES 30-60 (IEC = 1.2-2.2 meq g⁻¹) and SPSS 20-50 (IEC = 0.7-1.8 meq g⁻¹) membranes. The diffusion coefficient was found to increase with the IEC while solubility decreases. The results are discussed in the context of water/polymer interactions and morphology-facilitated mass transport characteristics.

© 2005 The Electrochemical Society. [DOI: 10.1149/1.1896529] All rights reserved.

Manuscript submitted July 7, 2004; revised manuscript received November 16, 2004. Available electronically May 11, 2005.

The current state-of-the-art proton exchange membrane fuel cell (PEMFC) technologies are based on perfluorinated sulfonic acid chemistry, *e.g.*, Nafion. Although an extraordinary longevity of over 60,000 h under fuel cell conditions has been achieved with commercial Nafion membranes, these materials remain expensive and have several limiting factors that restrict their application to below 100°C.¹ Increasing industrial interest in the application of nonfluorinated membranes as economically feasible alternatives to polymer electrolyte membranes (PEMs) for fuel cell operation has generated an abundance of research in the past decade. Primary requirements for these new materials are high proton conductivity, good thermochemical stability, and mechanical strength.²

Recently, the sulfonated poly(arylene ether sulfone) (SPES) family has been reported as a promising family of materials for elevated temperature fuel cell operation.³ Being well-known engineering thermoplastics, poly(arylene ether sulfone) (structure 1) displays a high glass transition temperature (T_g) of 195°C, good resistance to hydrolysis and oxidation, excellent mechanical properties, and high thermal stability.⁴ The closely related polyether sulfone (structure 2) is totally devoid of aliphatic hydrocarbon groups and exhibits even higher thermal stability ($T_g = 230^\circ\text{C}$).⁵ The introduction of sulfonate groups to the polyaromatic backbone not only produces enhanced intermolecular interaction by pendant ions but also increases molecular bulkiness, thus hindering internal rotation and leading to increased T_g for sulfonated copolymers.³ Impedance measurement by Benaventa *et al.*⁶ showed that sulfonation clearly affects the properties of the poly(arylene ether ether sulfone) family, particularly their water uptake, transport, and electrical parameters. Recently, direct polymerization of sulfonated poly(arylene ether sulfone) using sulfonated monomers has been reported.³ These polymers exhibit proton conductivity in excess of 0.08 S/cm (40% sulfonation level, 30°C, 100% RH) and good thermal stability ($T_g = 220\text{--}280^\circ\text{C}$), which meets the requirement for high-performance PEMFC.³ Another promising material is sulfonated poly(phenylene sulfide sulfone) (SPSS). The semicrystalline polymer, poly(phenylene sulfide) (PPS, Structure 3) has a T_g around 85°C and a T_m (crystalline transition temperature) of $\sim 285^\circ\text{C}$,^{7,8} with inherently high fire resistance and excellent solvent/chemical resistance. A related poly(phenylene sulfide sulfone) (PPSS, Structure 4) has been described in the literature as an amorphous polymer with a T_g around 217°C.⁹ Direct polymerization synthesis of SPSS has been reported¹⁰ and the proton conductivity of the fully hydrated membranes at 30°C was determined to be 0.05 and 0.06 S/cm for the 30 and 40 mol % sulfonated materials, respectively.¹¹

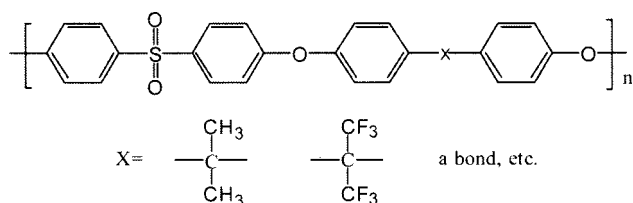
Compared to conventional perfluorosulfonate systems such as Nafion, these new hydrocarbon-based sulfonated copolymers represent a very different chemistry. Successful application of these new ion conducting copolymeric membranes in PEM fuel cells requires not only excellent proton conduction, but also efficient mass transport properties within the electrolyte. The challenge is that while the membrane cannot be too permeable to the reactive gases to prevent excessive gas crossover leading to loss of efficiency, the ionomer in the reaction layer of the gas diffusion electrode must have sufficient gas permeability so that the transport of dissolved reactant gases occurs without substantial concentration gradients and related mass transfer losses.¹²⁻¹⁴

In previous publications, mass transport parameters for the oxygen reduction reaction at the interface between Pt and a variety of solid-state perfluorosulfonic acid-type materials (Nafion and Aciplex membranes) have been studied.¹⁵ Mass transport characteristics in these membranes have been examined in terms of both environmental factors (temperature and pressure)¹⁶⁻¹⁸ as well as membrane structure and composition.¹² Similar investigations had been made on a series of sulfonated α , β , β -trifluorostyrene (BAM, Ballard, Canada) membranes and sulfonated styrene-(ethylene-butylene)-styrene triblock copolymers (DAIS, DAIS-Analytic, USA).¹⁸⁻²⁰ These studies suggested that oxygen transport behavior was primarily related to the water content in the PEM.

Water uptake of the membrane plays a critical role in the operation of a PEMFC; it affects various membrane properties including proton conductivity,²¹ methanol permeability,²² electro-osmotic drag,²³ as well as oxygen transport process.¹⁸ However, the degree of water absorption on a mass basis does not correlate well with those properties, especially when comparisons are made between different macromolecular systems.²⁴ We have recently reported oxygen permeation characteristics and interfacial kinetics for SPES-40 [40% sulfonated poly(arylene ether sulfone)], SPES-PS [sulfonated poly(arylene ether sulfone) - post sulfonated], and Nafion 117 membranes at the membrane/microelectrode interface as a function of various temperature and pressure conditions.^{14,25} In this report, SPES-40 and SPES-PS were found to have relatively low diffusion coefficients despite their higher water uptake (approximately twice the IEC). The pressure dependence of oxygen solubility showed an increasing trend for all the membranes, as expected, while the diffusion coefficient for the two SPES membranes showed an approximately linear increase with pressure. Changes in the microstructure of the membranes as a consequence of pressurization were proposed to be responsible for the variation of the diffusion coefficient with pressure. These results were discussed in the context of water content and microstructure of the membranes. The conformations of water-filled channels connecting the hydrophilic ionic clusters were found to have important contributions in the process of O₂ diffusion. The chemical composition of the SPES membrane was reported to

^a Present address: Gesellschaft zur Förderung von Medizin-, Bio- und Umwelttechnologien e.V., D-06132 Halle/Saale, Germany.

^z E-mail: smukerje@lynx.neu.edu



Structure 1. Poly(arylene ether sulfones).

be a major determinant in the observed mass transport properties of oxygen in these alternative polymer electrolyte systems given the relatively less pronounced hydrophobic hydrophilic nano-phase segregation of the SPES membrane as compared to the perfluorinated sulfonic acid polymer system of Nafion.

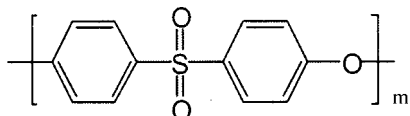
The present study focuses on investigating the oxygen transport properties of SPES and SPSS membranes as a function of copolymer sulfonation level. The principal goal here was to assess these polymers under environmental conditions (*i.e.*, temperature, pressure, and humidity) that mimic real fuel cell operations. In line with these objectives, this paper reports the variation of the oxygen transport parameters as a function of differences in polymer chemistry and morphology as well as changes in their respective ion exchange capacities. For this, a solid-state microelectrode method was employed using the well-established transient chronoamperometry technique in conjunction with a Pt microelectrode. This allowed for the direct measurement of both diffusion coefficient as well as solubility, the product of the two being the corresponding permeability. The parameters obtained were compared with a Nafion 117 membrane which was used as a control experiment.

Experimental

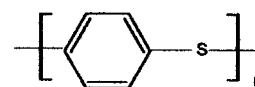
Membranes.—The sulfonated poly(arylene ether sulfone) polymers (SPES 30-60, Structure 5) used for this work were synthesized in-house in accordance with methodology described elsewhere;³ detailed preparation methodology, reaction conditions, and membrane properties, such as T_g , hydrophilicity, viscosity, TGA, AFM (hydrophilic domain size, phase inversion) and proton conductivity have been reported earlier.³ Sulfonated poly(arylene sulfide sulfone) (SPSS 20-50, Structure 6), were prepared by Foster-Miller, Inc. (Waltham, MA). Nafion 117 (Structure 7) was bought from Aldrich.

All membranes were soaked in 1 M sulfuric acid for 48 h at room temperature to ensure full protonation. After protonation, the membranes were rinsed several times and stored in deionized water. To determine the ion exchange capacity (IEC), a dried membrane sample was transferred to a flask and 50 mL of 3 M NaCl added. The membrane was stirred and equilibrated in the NaCl solution for 24 hrs and the solution was titrated with standardized 0.01 M NaOH using phenolphthalein as an indicator.

Water uptake measurements were carried out according to typical method reported earlier.^{26,27} Membranes were vacuum-dried at 100°C for 24 h then weighed, followed by immersion in deionized water at 30°C for 24 h. Following equilibration the wet membranes were quickly weighed, after removal of excess water prior to weighing. The water content in terms of wt% was determined as: $\text{H}_2\text{O}[\%] = [(\text{wet weight} - \text{dry weight}) / \text{dry weight}] \times 100\%$. The number of moles of water per sulfonic acid group ($\lambda = [\text{H}_2\text{O}] / \text{SO}_3^-$) was also calculated.



Structure 2. Polyether sulfone.



Structure 3. Poly(phenylene sulfide) (PPS).

Solid-state electrochemical cell setup and instrumentation.—The electrochemical cell setup designed to perform solid-state electrochemical experiments using a Pt microelectrode under controlled pressure, temperature, and relative humidity conditions has been described in detail earlier.^{14,25} Briefly, it consists of a 100 μm diam micro-disk Pt working electrode (Bioanalytical Systems Inc.), a solid-state dynamic hydrogen reference electrode (DHE), and a counter electrode, which are all on the same side of the membrane. Details of the setup and application of the transient chronoamperometric method for determination of oxygen permeability can be found elsewhere.^{14,25} A computer-controlled digital potentiostat/galvanostat (Autolab model, PGSTAT-30) was employed to conduct CV and chronoamperometry experiments.

Electrochemical techniques.—Fast scan CV (0.08-1.5 V) at a scan rate of 100 mVs^{-1} was performed during periods of equilibration at each condition for cleaning and activating the Pt microelectrode.

Chronoamperometry experiments were used to determine the diffusion coefficient and solubility of oxygen for the membranes. The experiments were performed by holding the potential of the microelectrode at 1.2 V for 20 s, then stepping to 0.4 V and holding for 5 s. Plotting of current, I , vs. the reciprocal of the square root of time, $t^{-1/2}$, for a time domain from 1 to 5 s gave a linear relationship corresponding to the modified Cottrell equation

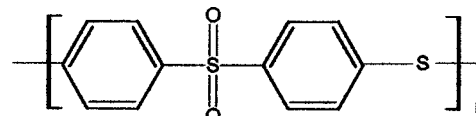
$$I(t) = \frac{nFAD^{1/2}C}{\pi^{1/2}t^{1/2}} + \pi FnDCr \quad [1]$$

where A is the geometric area of the microelectrode. D and C values were obtained simultaneously from linear regression analysis of the slope and intercept. For details on the choice of this equation and use of this methodology see Ref. 15-18. The activation energy of O_2 diffusion and enthalpy of dissolution of O_2 in the membranes were calculated according to

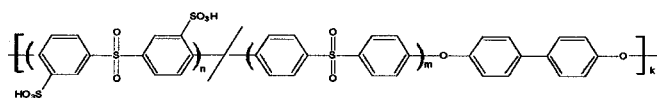
$$E_d = -2.303R \left[\frac{d \log D}{d(1/T)} \right] \quad [2]$$

$$\Delta H_s = -2.303R \left[\frac{d \log C}{d(1/T)} \right] \quad [3]$$

Experimental procedure.—Before each experiment, the Pt microelectrode was polished and pretreated as described in the literature.^{15,19} After incorporation into the cell, the membrane was equilibrated with humidified gas at 303 K and ambient pressure for at least 12 h. The temperature dependence studies of oxygen reduction and transport measurements were conducted at 100% relative humidity in a temperature range of 303-353 K and 3 atm pressure (O_2 , total pressure). The pressure dependence studies of oxygen reduction and transport characteristics were conducted at 323 K, 100% RH in a pressure range of 1-4 atm (O_2 , total pressure). Electrochemical measurements were made after equilibration at preferred temperature or pressure conditions for at least 2 h. All experiments



Structure 4. Poly(phenylene sulfide sulfone).

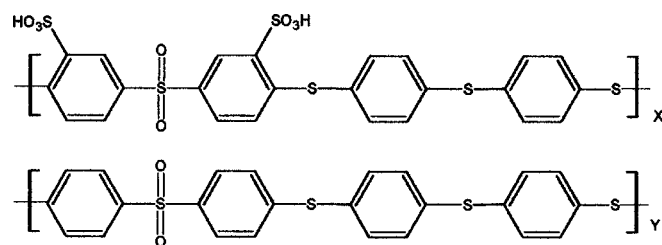


Structure 5. Sulfonated polyarylene ether sulfone SPES-XX (XX = 100n/n + m = 30 ~ 60).

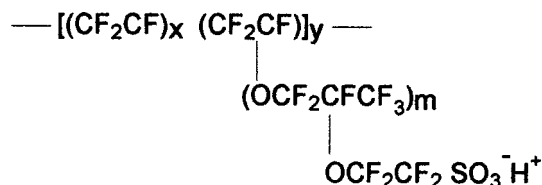
conducted for each of the membranes were repeated at least three times and the reproducibility monitored. All potentials stated here are relative to the DHE.

Result and Discussion

Effect of temperature and pressure on the O₂ transport properties.—Temperature dependence of O₂ transport parameters in SPES, SPSS, and Nafion 117 membranes were investigated over a range of 303 to 353 K at 3 atm oxygen pressure and 100% RH. The variation of diffusion coefficient (*D*) and solubility (*C*) with temperature are illustrated in Fig. 1 and 2. As expected, for all the membranes, *D* is observed to increase with temperature, while the opposite trend is true for *C*; however the increase in *D* with temperature is greater than the corresponding decrease in *C*, therefore the overall permeability (*D* × *C*) increases linearly with temperature. This increase appears to be more pronounced in high-IEC membranes within a structurally similar family of PEM, which is evident from the increase in the slope of the variation of *D* × *C* as a function of temperature as seen in the plots for SPES and SPSS membranes (Fig. 1 and 2). The trends of *D* and *C* with temperature are consistent with those previously reported and have been explained in great detail earlier.^{14,20,25} Plots of log *D* and log *C* vs. T⁻¹ shown in Fig. 3 and 4 exhibit a linear dependence over the temperature range investigated. Such a single linear variation with temperature allowed for unique activation energy values for O₂ diffusion (*E_d*) and the enthalpy of solubilization of O₂ in the membranes (*ΔH_s*) to be determined (Table I); these results are in good agreement with our previous reports on SPES-40 and SPES-PS membranes.^{14,25} The activation energy of O₂ diffusion (*E_d*) for SPES 20-60 (range of sulfonation, 20-60%) membranes ranges from 26 to 28 kJ mol⁻¹, which is close to Nafion 117 (26.5 kJ mol⁻¹). However, in SPSS 20-50 (range of sulfonation, 20-50%) membranes, a lowering of *E_d* (38.33 to 21.05 kJ mol⁻¹) with increased sulfonation content was observed. The exact reason for this is not clear, although Lee *et al.*⁴ recently reported a dependence of membrane cluster size on the activation energy for oxygen diffusion. Proper correlation of membrane morphology (in terms of changes in cluster size) and activation energy remains to be elucidated. The enthalpy of solubilization *ΔH_s* includes the heat of condensation and the heat of mixing.²⁸ A negative value for *ΔH_s* for oxygen dissolution can be regarded as an ordering process. As pointed out earlier,^{16,18} a negative value for oxygen dissolution can be expected based on negative entropy of dissolution in comparison phases which can be construed to be the extreme ends of the phases of Nafion (PTFE, nonaqueous phase and H₂SO₄, aqueous phase). Therefore, similar spatial arrangements of oxygen are expected be-



Structure 6. Sulfonated polysulfide sulfone SPSS-XX (XX = 100X/(X + Y) = 20-50).



Structure 7. Nafion 117.

tween the aqueous and nonaqueous components for Nafion 117, SPES, and SPSS membranes. *ΔH_s* for SPES 20-60 and SPSS20-50 membrane all showed a roughly increasing (less negative) trend with IEC values, which is most likely due to changes in morphology resulting from variations in ion exchange capacity and consequently changes in spatial rearrangements with respect to oxygen in the membranes. The exact mechanism of these interactions however awaits a molecular modeling study.

Pressure dependence of the gas transport parameters at a Pt/PEM interface was studied at 323 K as a function of O₂ pressure with the partial pressure of oxygen, PO₂, varying between 0.88 to 3.88 atm, corresponding to a total pressure range of 1 to 4 atm (after correction of saturated vapor pressure, 0.122 atm at 323 K @ 1 atm pressure). The variations of O₂ transport parameters with pressure are illustrated in Fig. 5 and 6 for SPES and SPSS membranes, respectively. Figures 5a and 6a show an increase of oxygen solubility *C* with pressure for all the membranes. Figures 5b and 6b display the plots of diffusion coefficient as a function of pressure. Two separate linear variations of *D* with pressure were found for Nafion 117 with a break at PO₂ of 1.5 atm; this consisted of an initial rapid increase for PO₂ < 1.5 atm, followed by a leveling off beyond 1.5 atm. For the SPES and SPSS membranes, the diffusion coefficient increased approximately linearly with pressure, in agreement with previously reported data by Basura *et al.*,²⁰ which was a similar investigation on BAM and DAIS membranes. These reproducible results on SPES and SPSS membranes are also consistent with our prior reports on SPES-40 and SPES-PS membranes, in which microstructure alteration, as well as polymer chain cooperative motions as a result of pressurization, were proposed to account for these phenomena.^{14,25}

As a consequence of the overall contributions from *D* and *C* as a function of pressure, the O₂ permeability (product of *D* × *C*) increases almost linearly with pressure (Fig. 5c and 6c).

Effect of copolymer composition on O₂ transport properties.—The experimentally determined ion exchange capacity (IEC) value reflects the actual amount of sulfonated groups incorporated into the copolymer; it is directly proportional to the degree of sulfonation. As shown in Table I, most of the SPES and SPSS copolymers have greater IEC values than Nafion 117, which are necessary to achieve comparable proton conductivities (*σ*) because the acidity of the aryl sulfonic acid is much weaker than the pendent perfluorosulfonic acid of Nafion.³ At a given temperature (*e.g.*, 30°C), water absorption in these sulfonated polyaromatic membranes increases with their IEC due to the strong hydrophilicity of the sulfonate group and an enhanced internal osmotic driving force in higher sulfonation polymers. The IEC of SPES and SPSS membranes studied here are in the range: 0.7 ~ 2.2 meq g⁻¹, falling in between their solubility and percolation limits. However, as in the case of SPES-60, whose water uptake at 30°C is as large as 161.1% (wt %), the copolymers with high degrees of sulfonation (>50%) tend to absorb excessive amounts of water and suffer from uncontrolled swelling and mechanical degradation. At 100% RH, 80°C and 3 atm O₂ pressure condition, SPES-60 became very soft and mechanically weak, therefore our experimental temperature on this membrane was limited to 70°C max.

Figure 7 plots the effect of IEC on diffusion coefficient, solubility, and permeability of oxygen for SPES, SPSS, and Nafion 117 membranes under three temperature conditions. The diffusion coef-

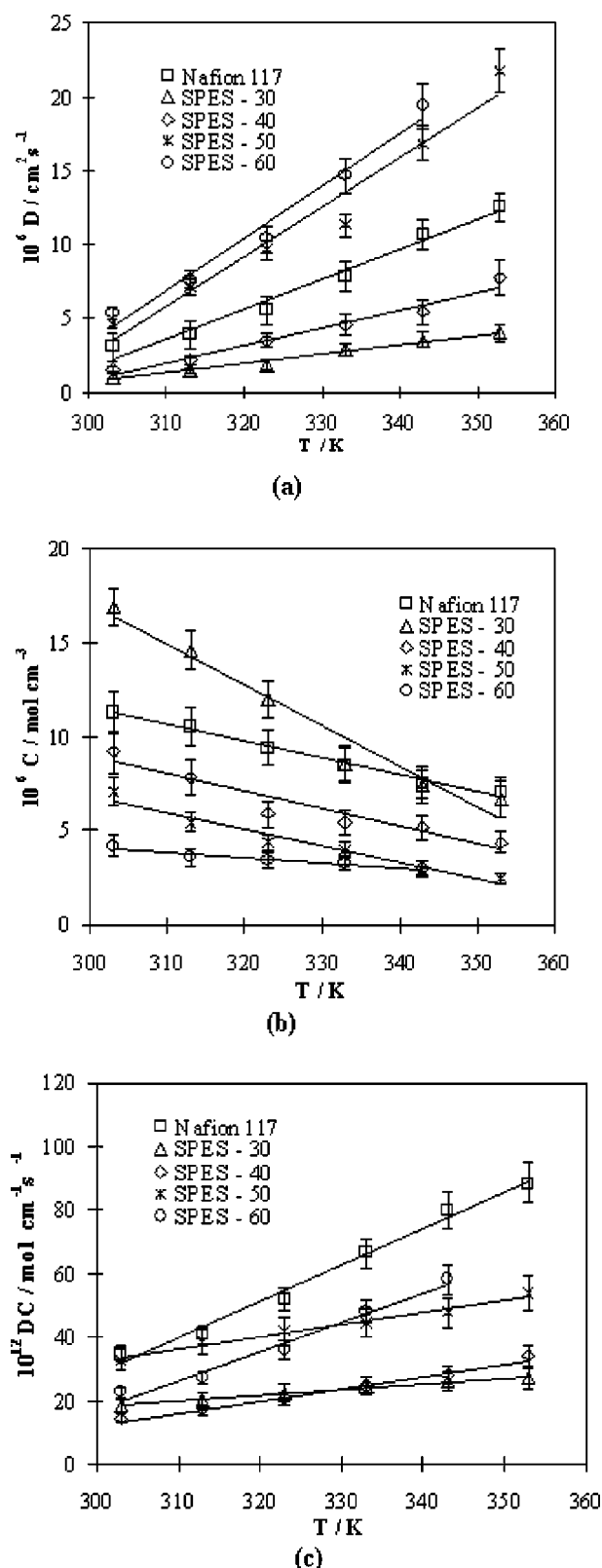


Figure 1. Effect of temperature on (a) diffusion coefficient (D) (b) solubility, (C) and (c) permeability ($D \times C$) for SPES membranes and Nafion 117 (control) in the range, 303-353 K, at 100% RH and 3 atm O_2 pressure.

coefficients of SPES and SPSS membranes exhibited an increase with increasing IEC, while the solubility correspondingly exhibited a decreasing trend. Similar trends have been observed earlier with perfluorinated materials (Nafion and Aciplex)¹² as well as BAM and DAIS membranes,²⁰ although the correlation of O_2 transport parameters with membrane compositions in these prior reports were made in terms of “equivalent weight” (weight of dry polymer in grams corresponding to one mole of exchange sites).

The IEC dependence of mass transport parameters can be simply interpreted on the basis of the water content of the fully hydrated membranes. It is widely accepted that the microstructure of perfluorosulfonate membranes such as Nafion is comprised of an amorphous hydrophilic phase containing the hydrated sulfonic acid sites, and partly crystalline hydrophobic Teflon backbone regions.²⁹⁻³¹ Both of these hydrophobic and hydrophilic phases have been described in prior research as having a strong impact on the electrochemical oxygen transport process:^{12,15,16,32} the aqueous domain (hydrophilic phase) is predominately involved in the O_2 diffusion pathway, hence more water uptake enables a higher diffusion coefficient of oxygen in the membrane. The solubility of oxygen was determined mainly by the fraction of the hydrophobic component in the membrane; as a result less water uptake and correspondingly relatively bigger fraction in the hydrophobic phase in the morphology tends to enhance O_2 solubility. Analogous correlation between membrane microstructure and electrochemical O_2 transport properties can be applied to sulfonated polyaromatic copolymers. TM-AFM imaging studies³ on SPES (referred to as BPSH-XX in previous literature) membranes has shown the existence of two roughly defined phases: the ionic cluster phase, comprised of hydrophilic sulfonic acid groups with associated hydration shells, and the non-ionic matrix phase assigned to the relatively hydrophobic aromatic backbone. For the SPSS copolymers, for which, to the best of our knowledge, there are no reported microstructure determinations published in literature, a similar phase separation into ionic/nonionic domains as those reported for SPES materials is expected to occur, taking into consideration their relatively similar chemical structures and identical trends for oxygen transport as a function of temperature. Prior reports have clearly correlated the increased water uptake as a consequence of higher ion exchange capacity with enlargement of the hydrophilic ionic domain.^{3,33} This is exemplified in a prior report³ where the TM-AFM (tapping mode atomic force microscopy) image of SPES-20 (IEC = 0.88) showed ionic clusters with diameters of 10-15 nm, in contrast to the ionic domain size of SPES-40 (IEC = 1.5), which increased to an ~ 25 nm diam. The extension of the aqueous phases facilitates the oxygen diffusion but results in lower O_2 solubility due to shrinking of hydrophobic zones.

However, aforementioned attempts to correlate oxygen transport parameters with proportional changes in hydrophilic/hydrophobic domains due to water absorption variations (with PEMs of different IEC used in this investigation) are not adequate. Comparison of oxygen transport parameters at 100% RH, 3 atm, and 323 K conditions for all the membranes provides for some interesting observations. As shown in Table I, despite the high water uptake and consequently bigger volume of aqueous phases in SPSS20-50 membranes, they all have smaller diffusion coefficients than Nafion 117. In the case of SPES membranes, the volume of aqueous phases in SPES-30 and SPES-40 are about 1.2-1.5 times greater than Nafion 117 but still have lower diffusion coefficients ($2.2 \text{ cm}^2 \text{ s}^{-1}$ for SPES-30, $3.52 \text{ cm}^2 \text{ s}^{-1}$ for SPES-40 vs. $5.51 \text{ cm}^2 \text{ s}^{-1}$ for Nafion 117); a sudden increase of diffusion coefficient occurs in SPES-50 and SPES-60 membrane, which are approximately three-fold higher than D in SPES-40 and almost double that in Nafion 117.

To interpret these results, it is essential to be aware of complications that can arise during the absorption and diffusion process of gas through the inhomogeneous sulfonated copolymer membrane system. According to a widely accepted theory by Vrentas and Duda,^{34,35} mass transport is mainly controlled by the availability of free volume within a system. Major physicochemical factors affecting the movement of gas in hydrated membranes include, the nature

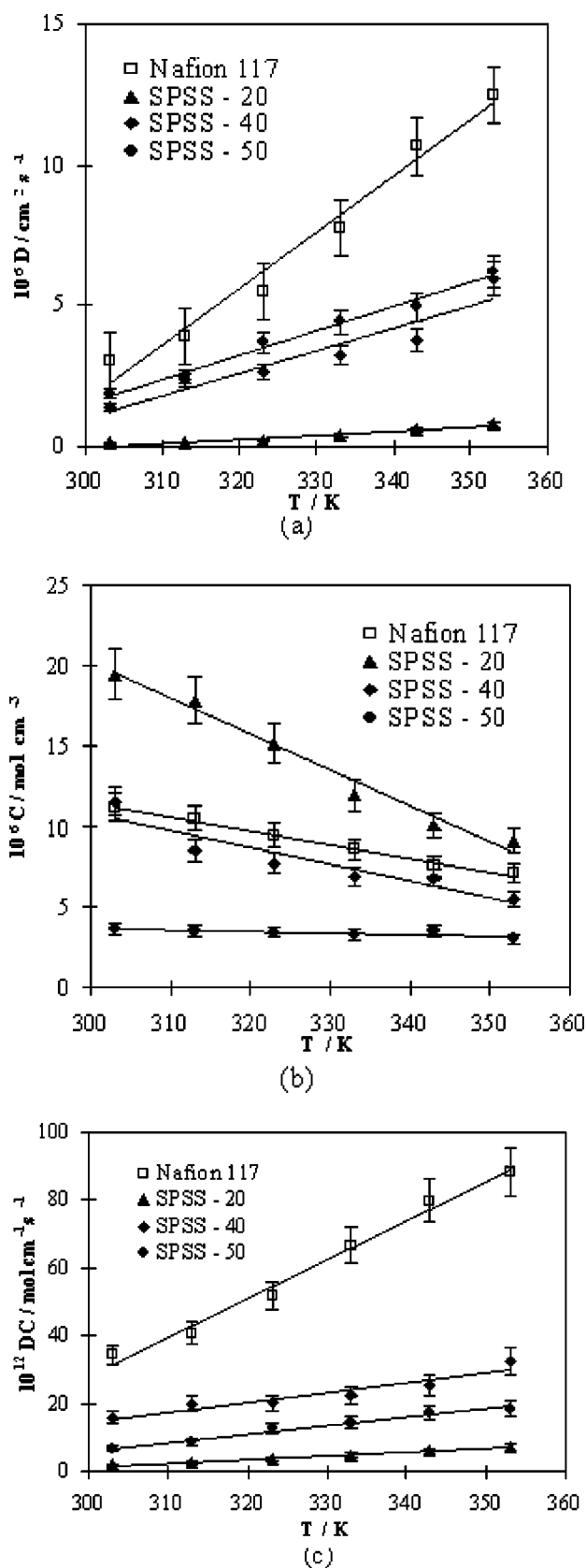


Figure 2. Effect of temperature on (a) diffusion coefficient (D) (b) solubility, (C) and (c) permeability ($D \times C$) for SPSS membranes and Nafion 117 (control) in the range 303–353 K, at 100% RH, and 3 atm O_2 pressure.

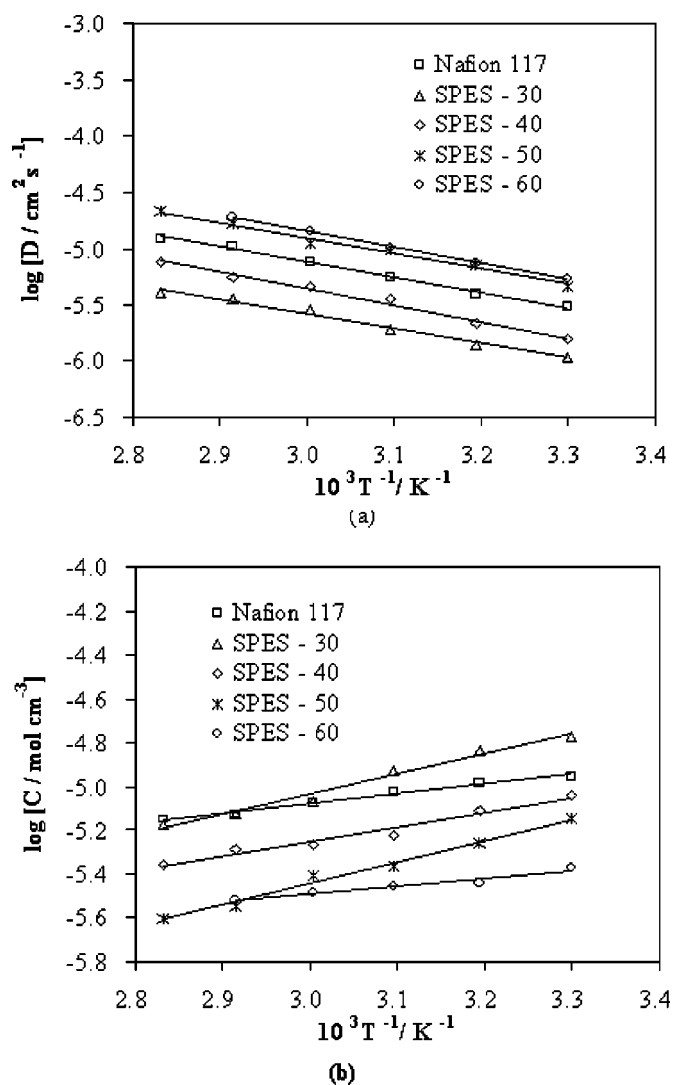


Figure 3. Arrhenius plots of (a) $\log D$ and (b) $\log C$ vs. $10^3 T^{-1}$ for SPES membranes under conditions of 100% RH, for a temperature range of 303–353 K, and 3 atm O_2 pressure (total pressure).

of the gas, the nature of the polymer, and the effects of various modifications of the polymer, such as crosslinking, plasticizing, crystallization, and varied filler materials.²⁸ Due to the small size of the O_2 molecule (reduced molecular diameter $\approx 2.5 \text{ \AA}$ ³⁶) and the relatively low gas concentrations encountered at normal pressures (below 10 bar), the gas's own contribution to its activated diffusion process in polymer membranes might be less evident.^{28,37} Thus O_2 permeation properties depend significantly on the polymer characteristics and water/polymer/solute (O_2) interactions. The former involves intra- and inter-chain flexibilities (e.g., cross-linking (if present), chain stiffness or T_g , crystallinity (if present), crystallite size, and distribution, etc.) and intrinsic molecular free volume (monomer repeat unit mass and distribution), etc.³⁸ The latter involves the hydrophilicity of the polymer and the states of water in the membrane; since water acts as a plasticizer in these membranes,^{24,39} the addition of the plasticizer to the polymer usually decrease the cohesive forces between the chains, resulting in an increase in segmental mobility²⁸ and therefore a depression of T_g in the fully hydrated membranes, as reported in a recent investigation regarding the state of water in SPES copolymers.²⁸ The movement of polymer segments gives rise to an increase in the free volume or vacant space (microvoid) into which a solute (O_2) can diffuse; conversely, the solute and the plasticizer may affect the segmental ther-

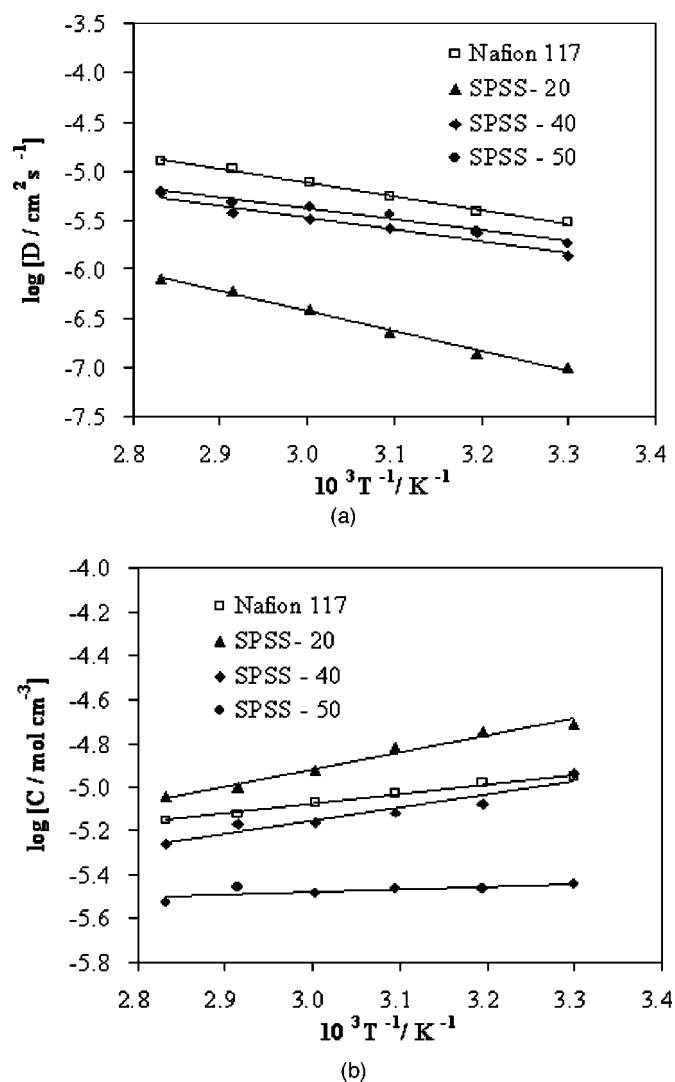


Figure 4. Arrhenius plots of (a) $\log D$ and (b) $\log C$ vs. $10^3 T^{-1}$ for SPSS membranes under conditions of 100% RH, for a temperature range of 303–353 K, and 3 atm O_2 pressure (total pressure).

mal motion by giving their own free volumes to the segment.⁴⁰ It is impossible to change one aspect of the whole gas/water/membrane system without affecting others. Therefore, interpretation of these factors requires advanced investigation by means of dynamic mechanical analysis (DMA), solid state NMR, molecular modeling techniques, etc.,^{38,41–43} which are beyond the scope of this paper. Nevertheless, based on our experiments there are several important points which are enumerated below.

First, the actual morphology of the hydrated membrane is the result of a combination of all concurrent physicochemical features; the gas transport behavior in the membrane is ultimately controlled by this morphology. As in the case of SPES membranes, there are remarkable differences in the SPES domain structure as a function of degree of sulfonation.³ As mentioned earlier, prior studies using TM-AFM images found that the ionic domain connectivity also varies depending on the degree of sulfonation:^{3,44} in SPES-20 the ionic cluster regions are isolated; in SPES-40 the phase contrast of the hydrophilic ionic domains increased though still being segregated; a significant change occurred in SPES-60 where the hydrophilic ionic domains became continuous, forming large channels of an ionic-rich phase. Such inherently larger and more “co-continuous” hydrophilic domains in higher IEC SPES membranes provide a faster transport pathway for O_2 ; hence they end up with higher diffusion coefficients. A similar continuous ionic channel structure was also observed in Nafion 117, although the domain size of the Nafion was reported to be 4–10 nm.³ The well-connected channels between ionic domains of Nafion 117 may form three-dimensional water networks, which seems a more favorable transport pathway for O_2 . This is why Nafion 117 has a comparatively low IEC (0.91 meq g^{-1}) and low water uptake but with a relatively high diffusion coefficient.^{14,25}

Second, water content is not an adequate index for correlation of mass transport behavior among different types of proton exchange membranes. Although the wealth of prior reports seems to emphasize the central role of water content in determining the O_2 permeation in membranes, our experimental data indicates that in nonfluorinated membranes small variations in chemistry such as the replacement of an ether linkage with sulfide among an otherwise close polyaromatic structure (and similar IEC and water uptake values), such as in SPSS and SPES copolymers at 40% and 50% degree of sulfonation, result in very different O_2 permeation parameters, not to mention Nafion 117, which has an extremely distinct perfluorinated backbone structure (see Table I). The unexpectedly smaller diffusion coefficients of SPSS 40–50 compared to the SPES 40–50 membranes may be attributed to their chemical structures. The ether link in SPES copolymers has the ability to induce flexibility into the backbone by virtue of its rotational freedom;⁴⁵ the sulfur bridge in SPSS probably plays a similar role but seems to provide for a dif-

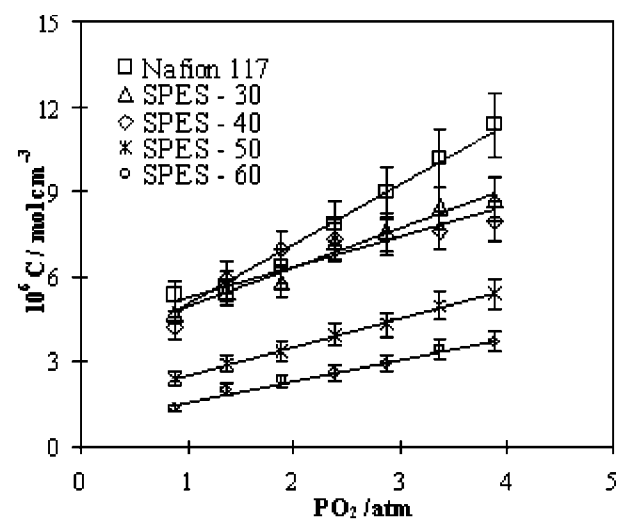
Table I. Comparison of O_2 transport parameters measured under conditions of 100% RH, 323 K, 3 atm O_2 pressure (total pressure) for various PEM systems. Also included are the corresponding data for ion exchange capacity, water uptake at 303 K, the volume of the aqueous phase as well as the values of the activation energy for oxygen diffusion and the enthalpy of dissolution.

| Membrane | IEC meq g^{-1} | Water uptake ^a wt% | Volume of aqueous phase ^b % | λ NO. of H_2O per SO_3H | σ^c (30°C) S cm^{-1} | Diffusion Coefficient $10^6 D$ $cm^2 s^{-1}$ | Solubility $10^6 C$ mol cm^{-3} | Permeability $10^{12} DC$ mol $cm^{-1} s^{-1}$ | E_d kJ mol^{-1} | ΔH_s kJ mol^{-1} |
|------------|---------------------|----------------------------------|--|--|----------------------------------|---|---|--|------------------------|-------------------------------|
| SPES-30 | 1.2 | 34.5 | 43.1 | 16 | 0.05 | 2.2 | 10.54 | 23.23 | 25.02 | -17.79 |
| SPES-40 | 1.5 | 47.3 | 51.0 | 17.5 | 0.084 | 3.52 | 5.92 | 20.83 | 28.18 | -12.89 |
| SPES-50 | 1.8 | 59.6 | 56.7 | 18.4 | 0.11 | 9.66 | 4.33 | 41.79 | 26.7 | -18.59 |
| SPES-60 | 2.2 | 161.1 | 78.0 | 40.7 | 0.17 | 10.34 | 3.47 | 35.91 | 28.03 | -6.71 |
| SPSS-20 | 0.7 | 24.6 | 35.1 | 19.5 | 0.024 | 0.22 | 15.21 | 3.40 | 38.33 | -14.66 |
| SPSS-40 | 1.5 | 71.5 | 61.1 | 26.5 | 0.072 | 2.62 | 7.69 | 20.17 | 22.72 | -11.59 |
| SPSS-50 | 1.8 | 102.6 | 69.3 | 31.7 | 0.08 | 3.69 | 3.41 | 12.61 | 21.05 | -2.46 |
| Nafion 117 | 0.9 | 20 | 30.6 | 12.5 | 0.12 | 5.51 | 9.42 | 51.88 | 26.5 | -8.73 |

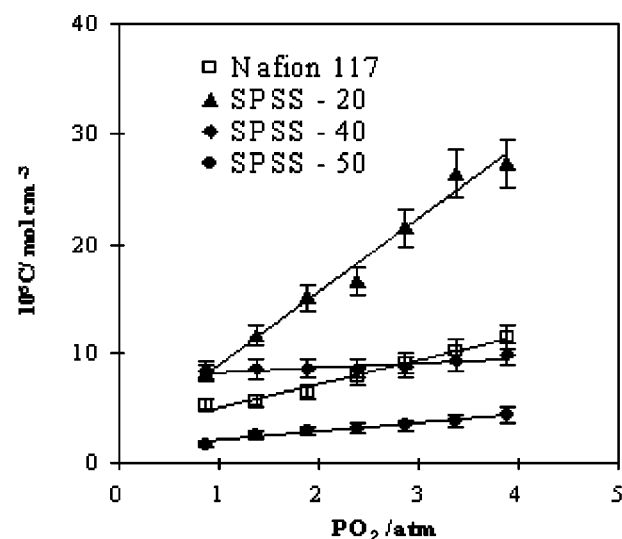
^a Swollen in water at 30°C.

^b Assuming a density of 2.2 $g cm^{-3}$ for the membrane phase and 1 $g cm^{-3}$ for the aqueous phase, allowing for no voids.

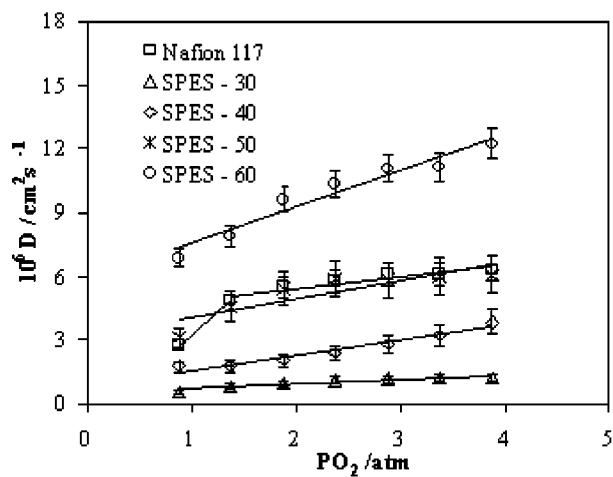
^c Data for SPES obtained from Ref. 3



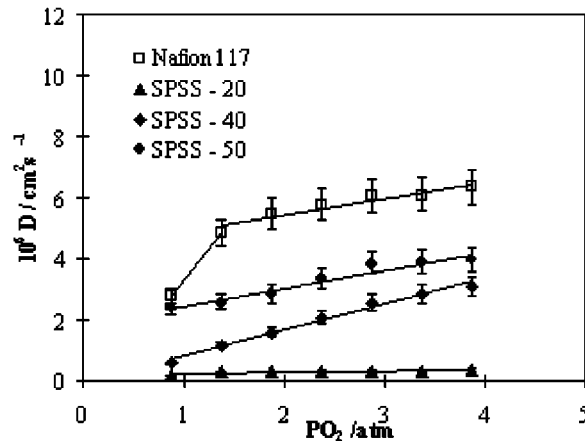
(a)



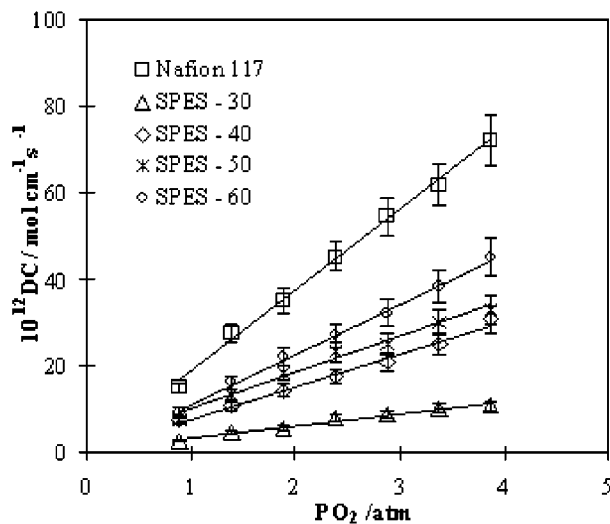
(a)



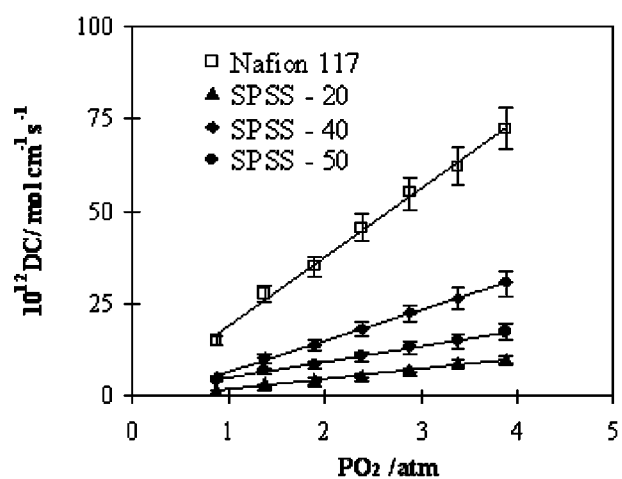
(b)



(b)



(c)



(c)

Figure 5. Effect of pressure on (a) solubility (C) (b) diffusion coefficient (D) and (c) permeability ($D \times C$) for SPES membranes and Nafion 117 (control) in the temperature range, 303-353K, 100% RH and 3 atm O_2 pressure.

Figure 6. Effect of pressure on (a) solubility (C) (b) diffusion coefficient (D) and (c) permeability ($D \times C$) for SPSS membranes and Nafion 117 (control) at 303-353 K, 100% RH, 3 atm O_2 pressure.

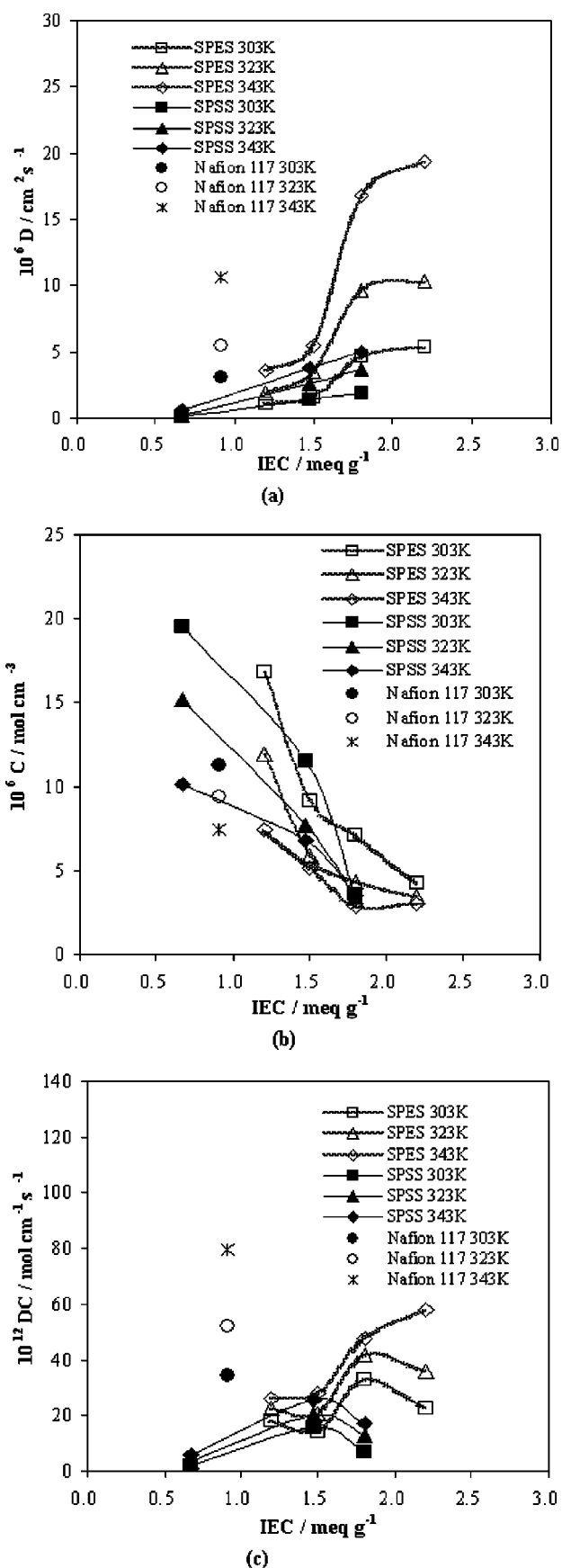


Figure 7. Effect of ion exchange capacity (IEC) on (a) diffusion coefficient (D) (b) solubility (C) and (c) permeability ($D \times C$) for SPES, SPSS membranes, and Nafion 117 (control) at 303, 323, and 343 K, 100% RH, 3 atm O₂ pressure.

ferent extent of chain stiffness. The introduction and distribution of polar side chains affects the cohesive energy²⁸ and consequently morphology of the polymer, which may also contribute to the slower gas migration in SPSS materials. Unfortunately, due to lack of an adequate morphological picture of SPSS, a quantitative correlation of O₂ permeability with the degree of sulfonation is not yet possible. Further characterizations are necessary to unveil the properties of these novel PEMs.

From the above discussion, we find that it is difficult to make comparisons of gaseous diffusion behavior among polymers of different structures, since the morphology can change drastically without appreciable changes in density. The presence of water and the hydrogen bonds formed between polymer-water moieties also have major effects on system properties. The magnitude and distribution of these hydrogen bonds causes consequent changes in the polymer structure, local chain segmental mobilities, and free volume content and its distribution.⁴⁶ There has been very little work reported on the effects of plasticization or absorbed water and chemical structure on the gas transport in proton exchange membranes. Much more detailed work on the polymer characterization and gaseous diffusion itself must be carried out before a full understanding of these effects is possible.

Finally, the permeability of oxygen reflects the overall contributions of diffusion and solubility of oxygen in the ionomer membranes. As shown in Fig. 7c, the oxygen permeability of the SPES and SPSS membranes increases with increasing IEC at lower sulfonation levels, which appears to reach a maximum value at intermediate sulfonation levels, followed by a drop; this is true at almost all temperature conditions in this work. Attention may be drawn here to the highly sulfonated nonfluorinated membranes, whose lower oxygen permeability and relatively poor mechanical strength cancel out their higher proton-conducting properties. Special care should be taken while choosing appropriate sulfonation levels for these new ionomers in order to achieve optimum performance.

Conclusions

Mass transport properties were determined for a series of sulfonated poly(arylene ether sulfone) (SPES) membranes and sulfonated polysulfide sulfone (SPSS) polymers of various ion exchange capacities (IEC) at a Pt (microelectrode)/proton exchange membrane (PEM) interface. The temperature and pressure dependence of oxygen transport parameters show similar trends for the SPES 30-60 (IEC = 1.2-2.2 meq g⁻¹) and SPSS 20-50 (IEC = 0.7-1.8 meq g⁻¹) membranes. The diffusion coefficient (D) was found to increase with IEC, while solubility (C) decreases. These results are discussed in the context of water content and microstructure of the membranes. The conformations of water-filled channels connecting the hydrophilic ionic clusters appear to have important contributions to the process of O₂ diffusion. Samples of SPES and SPSS polymers of various sulfonation levels vary in their diffusion coefficient and solubility even when they have the similar chemical composition due to inevitable differences in their morphology. The results of these studies emphasize the marked dependence of transport properties on subtle variations in polymer composition and structure.

Acknowledgments

The research presented in this paper was supported by the U.S. Department of Energy through a subcontract from Los Alamos National Laboratory. The authors thank Dr. David Ofer at Foster-Miller, Inc. (Waltham, MA) for providing SPSS membranes used in this work.

Northeastern University assisted in meeting the publication costs of this article.

References

1. M. Rikukawa and K. Sanui, *Prog. Polym. Sci.*, **25**, 1463 (2000).
2. J. Roziere and D. J. Jones, *Annu. Rev. Mater. Sci.*, **33**, 503 (2003).
3. F. Wang, M. Hickner, Y. S. Kim, T. A. Zawodzinski, and J. E. McGrath, *J. Membr.*

- Sci.*, **197**, 231 (2002).
4. R. E. Kesting, *Synthetic Polymeric Membranes: A Structural Perspective*, John Wiley & Sons, New York (1985).
 5. M. R. Pereira and J. Yarwood, *J. Chem. Soc., Faraday Trans.*, **92**, 2731 (1996).
 6. J. Benavente, A. Canas, M. J. Ariza, A. E. Lozano, and J. de Abajo, *Solid State Ionics*, **145**, 53 (2001).
 7. L. C. Lopez and G. L. Wilkes, *J. Macromol. Sci., Rev. Macromol. Chem. Phys.*, **29**, 83 (1989).
 8. J. F. Geibel and R. W. Campbell, in *Comprehensive Polymer Science Volume 5: Step Polymerization*, G. C. Eastmond, A. Ledwith, S. Russo, and P. Sigwalt, Editors, p. 543, Pergamon Press, Oxford (1989).
 9. R. W. Campbell, *Aromatic Sulfide/Sulfone Polymers*, Phillips Petroleum (1977).
 10. F. Wang, J. Mecham, W. Harrison, and J. E. McGrath, *Polym. Prepr. (Am. Chem. Soc. Div. Polym. Chem.)*, **41**, 1401 (2000).
 11. K. B. Wiles, V. A. Bhanu, F. Wang, and J. E. McGrath, Paper POLY010 presented at the ACS National Meeting, Boston, MA 2002.
 12. F. N. Buechli, M. Wakizoe, and S. Srinivasan, *J. Electrochem. Soc.*, **143**, 927 (1996).
 13. T. E. Springer, M. S. Wilson, and S. Gottesfeld, *J. Electrochem. Soc.*, **140**, 3513 (1993).
 14. L. Zhang, C. Ma, and S. Mukerjee, *Electrochim. Acta*, **48**, 1845 (2003).
 15. A. Parthasarathy, C. R. Martin, and S. Srinivasan, *J. Electrochem. Soc.*, **138**, 916 (1991).
 16. A. Parthasarathy, S. Srinivasan, and A. J. Appleby, *J. Electrochem. Soc.*, **139**, 2530 (1992).
 17. A. Parthasarathy, S. Srinivasan, A. J. Appleby, and C. R. Martin, *J. Electrochem. Soc.*, **139**, 2856 (1992).
 18. P. D. Beattie, V. I. Basura, and S. Holdcroft, *J. Electroanal. Chem.*, **468**, 180 (1999).
 19. V. I. Basura, P. D. Beattie, and S. Holdcroft, *J. Electroanal. Chem.*, **458**, 1 (1998).
 20. V. I. Basura, C. Chuy, P. D. Beattie, and S. Holdcroft, *J. Electroanal. Chem.*, **501**, 77 (2001).
 21. R. W. Kopitzke, C. A. Linkous, H. R. Anderson, and G. L. Nelson, *J. Electrochem. Soc.*, **147**, 1677 (2000).
 22. J. Kim, B. Kim, and B. Jung, *J. Membr. Sci.*, **207**, 129 (2002).
 23. X. Ren and S. Gottesfeld, *J. Electrochem. Soc.*, **148**, A87 (2001).
 24. Y. S. Kim, L. Dong, M. A. Hickner, T. E. Glass, V. Webb, and J. E. McGrath, *Macromolecules*, **36**, 6281 (2003).
 25. L. Zhang, C. Ma, and S. Mukerjee, *J. Electroanal. Chem.*, **568**, 273 (2004).
 26. T. A. Zawodzinski, Jr., T. E. Springer, J. Davey, R. Jestel, C. Lopez, J. Valerio, and S. Gottesfeld, *J. Electrochem. Soc.*, **140**, 1981 (1993).
 27. K. Lee, A. Ishihara, S. Mitsushima, N. Kamiya, and K.-i. Ota, *J. Electrochem. Soc.*, **151**, A639 (2004).
 28. J. Crank and G. S. Park, *Diffusion in Polymers*, Academic Press Inc., London (1968).
 29. T. D. Gierke, G. E. Munn, and F. C. Wilson, *J. Polym. Sci., Polym. Phys. Ed.*, **19**, 1687 (1981).
 30. E. J. Roche, M. Pineri, R. Duplessix, and A. M. Levelut, *J. Polym. Sci., Polym. Phys. Ed.*, **19**, 1 (1981).
 31. S. C. Yeo and A. Eisenberg, *J. Appl. Polym. Sci.*, **21**, 875 (1977).
 32. P. C. Lee and M. A. J. Rodgers, *J. Phys. Chem.*, **88**, 4385 (1984).
 33. Y. S. Kim, F. Wang, M. Hickner, S. McCartney, Y. T. Hong, W. Harrison, T. A. Zawodzinski, and J. E. McGrath, *J. Polym. Sci., Part B: Polym. Phys.*, **41**, 2816 (2003).
 34. J. S. Vrentas and J. L. Duda, *J. Polym. Sci., Polym. Phys. Ed.*, **15**, 403 (1977).
 35. J. S. Vrentas and J. L. Duda, *J. Polym. Sci., Polym. Phys. Ed.*, **15**, 417 (1977).
 36. A. S. Michaels and H. J. Bixler, *J. Polym. Sci.*, **50**, 413 (1961).
 37. K. J. Lee, J. Y. Jho, Y. S. Kang, Y. Dai, G. P. Robertson, M. D. Guiver, and J. Won, *J. Membr. Sci.*, **212**, 147 (2003).
 38. H. C. Patel, J. S. Tokarski, and A. J. Hopfinger, *Pharm. Res.*, **14**, 1349 (1997).
 39. R. B. Moore III and C. R. Martin, *Macromolecules*, **21**, 1334 (1988).
 40. P. Neogi, *Diffusion in Polymers*, Marcel Dekker, Inc., New York (1996).
 41. M. D. Sefcik, J. Schaefer, F. L. May, D. Raucher, and S. M. Dub, *J. Polym. Sci., Polym. Lett. Ed.*, **21**, 1041 (1983).
 42. J. Schaefer, M. D. Sefcik, E. O. Stejskal, R. A. McKay, W. T. Dixon, and R. E. Cais, *Macromolecules*, **17**, 1107 (1984).
 43. S.-Y. Kwak, *Polymer*, **40**, 6361 (1999).
 44. Y. S. Kim, F. Wang, M. Hickner, S. McCartney, Y. T. Hong, W. Harrison, T. A. Zawodzinski, and J. E. McGrath, *J. Polym. Sci., Part B: Polym. Phys.*, **41**, 2816 (2003).
 45. P. E. Cassidy, *Thermally Stable Polymers: Synthesis and Properties*, Marcel Dekker, Inc., New York (1980).
 46. C. E. Rogers, J. R. Semancik, and S. Kapur, in *Transport Processes in Polymers*, R. W. Lenz and R. S. Stein, Editors, p. 297, Plenum Press, New York (1973).